

Neuronal correlates of real and illusory contour perception: functional anatomy with PET

Jonas Larsson, Katrin Amunts,¹ Balázs Gulyás, Aleksandar Malikovic,¹ Karl Zilles¹ and Per E. Roland

Division of Human Brain Research, Department of Neuroscience, Karolinska Institute, S-171 77 Stockholm, Sweden

¹Department of Anatomy and C. and O. Vogt Institute for Brain Research, Heinrich-Heine University, P.O. Box 101007, 40001 Düsseldorf, Germany

Keywords: extrastriate, form perception, neuroimaging, vision, visual cortex

Abstract

Illusory contours provide a striking example of the visual system's ability to extract a meaningful representation of the surroundings from fragmented visual stimuli. Psychophysical and neurophysiological data suggest that illusory contours are processed in early visual cortical areas, and neuroimaging studies in humans have shown that Kanizsa-type illusory contours activate early retinotopic visual areas that are also activated by real contours. It is not known whether other types of illusory contours are processed by the same mechanisms, nor is it clear to what extent attentional effects may have influenced these results, as no attempt was made to match the salience of real and illusory stimuli in previous imaging studies. It therefore remains an open question whether there are any brain regions specifically involved in the perception of illusory contours. To address these questions, we have used ¹⁵O-butanol positron emission tomography (PET) and a novel kind of illusory contour stimulus that is induced only by aligned line ends. By employing a form discrimination task that was matched for attention and stimulus salience across conditions we were able to directly contrast perception of real and illusory contours. We found that the regions activated by illusory contour perception were the same as those activated by real contours. Only one region, located in the right fusiform gyrus, was significantly more strongly activated by perception of illusory contours than by real contours. In addition, a principal component analysis suggested that illusory contour perception is associated with a change in the correlation between V1 and V2. We conclude that different kinds of illusory contours are processed by the same cortical regions and that these regions overlap extensively with those involved in processing of real contours. At the regional level, perception of illusory contours thus appears to differ from perception of real contours by the degree of involvement of higher visual areas as well as by the nature of interaction between early visual areas.

Introduction

Illusory contours have attracted considerable interest in recent years as probes for exploring mechanisms of figure–ground segregation and perceptual grouping. Illusory contours are usually perceived as sharp boundaries between regions which in reality do not differ in luminance or colour. Because contours are believed to be extracted at an early stage of visual processing, this dissociation between the physical stimulus and the resulting percept makes illusory contours a useful tool for locating where in the brain visual information is first transformed from a one-to-one map of the retinal stimulus into a representation that corresponds to the perception of the visual world. In natural scenes, occlusion cues similar to those that induce illusory contours often provide more reliable information about object shape than is given by luminance or colour cues alone. An understanding of the neural mechanisms of illusory contour perception could therefore in principle give insight into the processes that enable humans and other primates to segment visual scenes into their constituent objects.

Although early psychophysical studies of contour perception focused on high-level cognitive mechanisms to explain the perception of illusory contours, the last decades have witnessed a growing emphasis on bottom-up processes. The notion that bottom-up

mechanisms may suffice to explain illusory contour perception is supported by several lines of evidence: cats and monkeys are known to perceive illusory contours (Bravo *et al.*, 1988); real and illusory contours have similar perceptual effects (Smith & Over, 1979; Vogels & Orban, 1987; Paradiso *et al.*, 1989; Berkley *et al.*, 1994; Dresch & Bonnet, 1995); perception of at least certain kinds of illusory contours is preattentive (Gurnsey *et al.*, 1992); and many orientation-selective neurons in monkey V2 also respond to illusory contours along the same orientation (von der Heydt *et al.*, 1984; Peterhans & von der Heydt, 1991).

The question whether neuronal processing of illusory contours is purely bottom-up or also relies on cognitive factors has recently been investigated using neuroimaging methods. Hypothesizing that cognitive processes influencing illusory contour perception would be reflected in increased activity in the prefrontal cortex, neither Hirsch *et al.* (1995) nor ffytche & Zeki (1996) found any evidence of such increases. Although negative results in functional neuroimaging are inconclusive, these results are consistent with the bottom-up view of illusory contour processing in the sense that prefrontal regions do not seem to be strongly involved. This raises the question, however, of where such bottom-up processing takes place and whether the site and/or mechanisms of illusory contour perception differ from those involved in the perception of real (luminance- or colour-defined) contours. The evidence so far points to regions of extrastriate visual cortex, although the results of different studies are somewhat

Correspondence: Dr J. Larsson, as above.
E-mail: Jonas.Larsson@neuro.ki.se

divergent. Using functional magnetic resonance imaging (fMRI), Hirsch *et al.* (1995) found that illusory contours activated regions of extrastriate cortex primarily in the right hemisphere that were not activated by a control stimulus or by real contours. Similarly, ffytche & Zeki (1996) investigated illusory contour perception with positron emission tomography (PET) and found that it gave rise to increased blood flow in the extrastriate cortex that may correspond to V2 and adjacent visual areas. More recently, Mendola *et al.* (1999) have used fMRI and cortical surface-based analysis techniques to study illusory and real contour perception. With this method they were able to demonstrate that an illusory shape activates retinotopic visual areas in a manner that is similar to a shape defined by real contours, but also activates regions beyond the retinotopic areas that are not activated by luminance-defined contours. Because the field of view did not extend beyond the occipital cortex they were unable to address the issue whether illusory contours activate prefrontal regions.

Although these studies have addressed some of the issues regarding the neural basis of illusory contour perception, several questions remain unanswered. First, in none of the above studies was illusory and real contour perception directly contrasted in the same individual; instead different control stimuli for each type of stimulus were used and the resulting activations compared. This makes it difficult to claim with certainty that the regions activated by illusory contours are truly specific to this type of contour. While ffytche & Zeki (1996) did attempt to compare real and illusory contours directly (and found no significant difference between the two conditions), this comparison was made between two different groups of subjects. It is quite possible that the large residual variability introduced by this procedure masked any true difference between the conditions.

Second, no attempt was made to control for differences in attentional level in these studies. In one study (ffytche & Zeki, 1996) subjects were told to scan the stimuli in a learned sequence, but the performance of the subjects across conditions was not monitored. Because it is well known that visual attention can strongly modulate blood flow in extrastriate visual areas (Corbetta *et al.*, 1990, 1991a,b; Wojciulik *et al.*, 1998), one cannot exclude the possibility that the illusory contour-related activity observed in these studies is due to subjects attending more strongly to illusory contours than to real ones, especially as real and illusory contours can differ greatly in salience.

Third, it is not known whether different kinds of illusory contours are processed by the same cortical mechanisms. Previous functional neuroimaging studies have mostly used Kanizsa-type illusory contour stimuli, which differ in some important respects from the other major category of illusory contour, which is induced by aligned line ends (e.g. by phase-shifted abutting gratings). Kanizsa-type illusory contours are induced parallel to an inducing shape, in effect as an extension of an invisible occluding contour, whereas illusory contours formed by aligned line ends are induced perpendicular to the inducing lines. Illusory contours formed by abutting gratings have been shown to be detected preattentively (Gurnsey *et al.*, 1992); opinions differ whether this is also the case for Kanizsa-type illusory contours (Davis & Driver, 1994; Gurnsey *et al.*, 1996). The salience of the abutting grating type of illusory contour is determined primarily by local features, e.g. the shape of the tips of the inducer lines (Soriano *et al.*, 1996), whereas the salience of Kanizsa-type illusory contours is much more sensitive to global parameters, e.g. the shape of the inducers or the presence of distractors (Fig. 1a and b). Further, for a given support ratio, the ratio of inducing contour length to total illusory contour length (Shipley & Kellman, 1992), illusory contours created by aligned line ends are usually perceived as more salient than the Kanizsa type, at least when the support ratio is low

(Fig. 1b). Although these differences do not necessarily rule out a common cortical locus for illusory contour perception, the two types of contour rely on different types of visual grouping mechanisms. To account for these differences, models of illusory contour perception generally postulate two separate mechanisms—one integrating responses along inducer orientation, the other integrating responses perpendicular to this orientation—that feed into the same ‘contour’ processing system (Peterhans & von der Heydt, 1989; von der Heydt & Peterhans, 1989; Heitger *et al.*, 1992; Grossberg, 1994). Whether these two mechanisms also correspond to spatially distinct neuronal populations is not clear. Mendola *et al.* (1999) used illusory contour stimuli created by phase-shifted gratings and found that this type of stimulus did not activate early retinotopic areas as strongly as Kanizsa-type contours. However, a confound of the phase-shifted grating is that the phase shift itself creates a texture difference that may have contributed to the observed signal. Ideally, a true illusory contour stimulus should be defined only by the illusory contour and not be detectable by any other means.

This study was designed to address these unresolved issues. First, by directly contrasting real and illusory contour conditions we were able to identify regions truly specific to either kind of stimulus. Second, by using a task that was identical for both conditions we could control behavioural attention level, as a way of matching the level of visual attentional modulation between conditions. Third, by using a new type of illusory contour stimulus defined entirely by aligned line ends we could selectively stimulate the end-stopped cell population believed to underlie the perception of such contours independent of the confounding texture component created by a grating.

Materials and methods

Tasks

Subjects were scanned during three conditions: while performing a visual form discrimination task in which forms were defined either by luminance contrast (‘real’) contours (real condition) or illusory contours (illusory condition), and while performing a visual control task (fixation condition). In the form discrimination conditions subjects viewed three simultaneously presented elliptical or circular shapes side by side and had to determine which one differed from the other two by being more or less elliptical. The orientation of the ellipses was random. The different shape was always located to the left or to the right of the middle and subjects responded by pressing one of two mouse buttons. Each trial was preceded by display of a fixation point for 300 ms, followed by the stimulus display for 1500 ms, followed by a blank screen for 200 ms. Subjects were instructed to respond as quickly and accurately as possible. To avoid confounding effects of eye movements, subjects were required to maintain their gaze on the fixation point in the centre of the display and to minimize their eye movements while viewing the stimuli, restricting any such movements to the central field of view ($\sim 5^\circ$). Because real and illusory stimuli were of identical dimensions and matched for salience, eye movements should not differ between these conditions. In the fixation condition, subjects responded to the appearance of the fixation point only, which was followed by a blank screen for 1700 ms, so that the number of responses during both tasks and control was identical. Stimuli were displayed and responses collected using ERTS software (BeriSoft, Frankfurt, Germany) on a computer monitor covering $16 \times 12^\circ$ of the visual field. Mean luminance of the inducing lines was 14.1 cdm^{-2} and the background luminance was 0.7 cdm^{-2} , corresponding to 91% contrast. In the visual form task, the shapes had a mean diameter of 3° and were

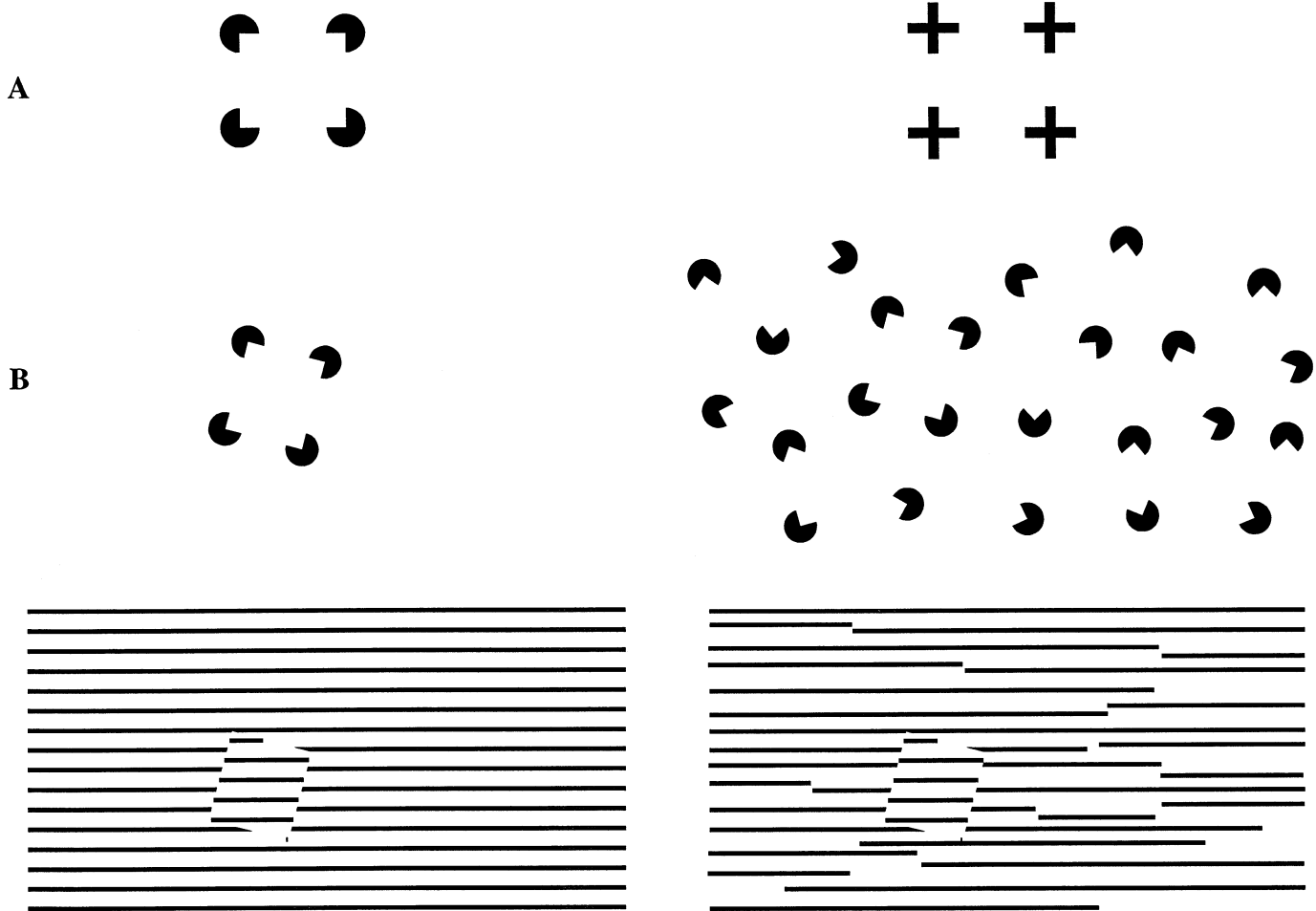


FIG. 1. Differences between illusory forms formed by aligned line ends and Kanizsa figures. (a) Sensitivity of Kanizsa-type illusory contours to global inducer shape. An illusory shape is only perceived in the left figure, even though the inducing contours are identical in the left and right figures. This suggests that perception of Kanizsa-type contours requires the formation of a global form percept rather than being purely driven by configuration of local features. (b) Saliency of illusory contours formed by aligned line ends versus Kanizsa figures. On the left, the saliency of the illusory rectangle is generally perceived as stronger in the lower figures even though the support ratio (ratio of interpolated contour to total illusory contour length) is the same in both the upper and lower panels. On the right, addition of distractors reduces the saliency of the Kanizsa-type illusory shape more than that of the rectangle formed by abutting gratings, suggesting stronger dependence on global configuration for Kanizsa-type illusory contours.

located at the centre, and 5.5° to the left and right of the centre of the display, respectively. The total visual angle subtended by the stimuli was $\sim 14 \times 3.5^\circ$. The shapes used in the form task were embedded in a background matrix of randomly oriented lines (length $0.3\text{--}0.9^\circ$, width 0.04°) that covered the entire display. In the real condition, the shapes were defined by thin (0.02° wide) line contours. In the illusory condition, the shapes were defined by illusory contours created by arranging a subset of the background lines so that their tips were aligned at one end (Fig. 2). (We have found that the saliency of this type of illusory contour is strongly related to viewing parameters, especially the contrast and size of the inducing line ends. To perceive the stimulus as closely to that used in this study the reader should view each panel of Fig. 2 so that it subtends $16 \times 12^\circ$ of the visual angle.) To roughly equate the saliency of this stimulus to that of the real contour stimulus we varied the stimulus parameters for the illusory contours until the times required to detect a randomly located illusory shape and an equivalent real shape were equal. The saliency of illusory contours formed by aligned line ends has been shown to be strongly reduced if the orientation of the inducer lines deviates more than $\sim 30^\circ$ from a direction perpendicular to the induced contour (Soriano *et al.*, 1996). For this reason, the orientation between the

inducer lines and the induced contour was restricted to be between 75 and 105° . The weak radial texture pattern that may be perceived as a result of this constraint could in principle obscure the illusory component of the task in a manner analogous to the phase shift confound of an abutting grating-type illusory contour. To establish that the task did indeed rely on perception of illusory contours we tested two subjects on their performance of the task using stimuli with illusory contours compared with stimuli where the illusory contours had been removed by randomly shifting the inducer lines towards or away from the induced contour. The result of this test is shown in Fig. 3. As is apparent, there was a significant (F ratio = 5.88 , $P < 0.02$) drop in performance for both subjects when the illusory contours were removed, even though the radial component remained unchanged. Thus, any regional cerebral blood flow (rCBF) changes related to the illusory condition were unlikely to be due to textural effects.

Scanning procedure

Six male subjects (mean age 28.2 years, range 22–39 years) participated in the study. They were informed of the risks involved and gave their consent to participate in accordance with the

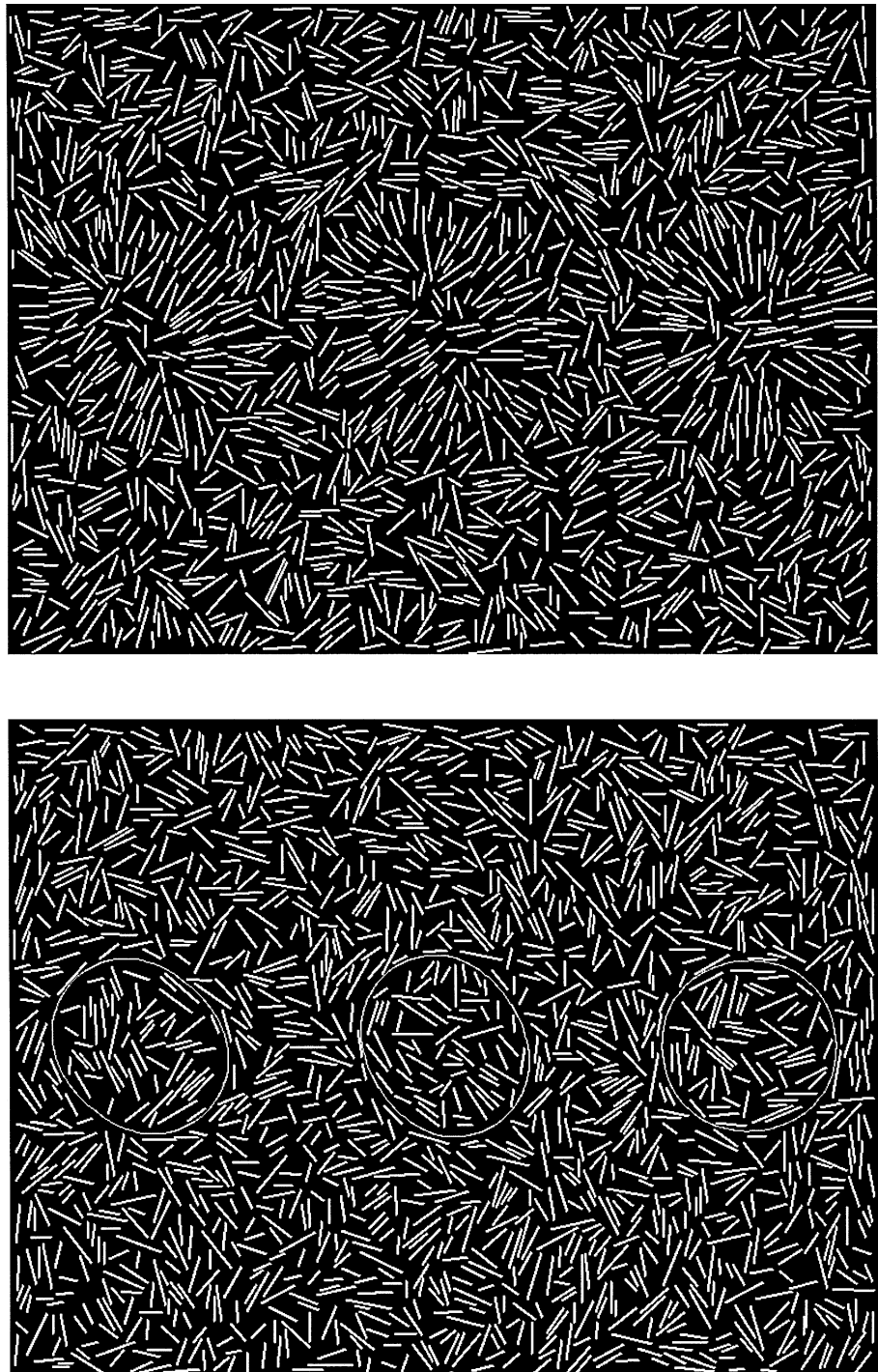


FIG. 2. Examples of stimuli used in the illusory condition (top) and the real condition (bottom). Subjects had to decide whether the odd shape out was located to the left or right of the middle. The display used in the experiment subtended $16 \times 12^\circ$ of visual angle.

guidelines of the Helsinki declaration. The study was approved by the Ethics Committee of the Karolinska Institute and Hospital. Prior to the PET scanning session, a T1-weighted high-resolution anatomical magnetic resonance (MR) scan (GE Signa 1.5 T, SPGR) was made of each subject's brain. Head fixation was provided by an individually moulded plastic helmet, which was also used in the PET scan session. A total of 12 scans were made on each subject, each condition repeated four times in blocks. The order of conditions was randomized within each block. rCBF was measured with an ECAT EXACT HR PET scanner in three-dimensional mode. ^{15}O -butanol was used as tracer (14 mCi per scan). The arterial tracer concentration was monitored continuously with an automatic blood sampler system,

and used to calculate the rCBF using an autoradiographic method (Meyer, 1989). The PET images were filtered with a Gaussian kernel with a full width at half maximum of 8 mm prior to blood flow calculation, and subsequently normalized to a global blood flow of 50 mL/100 mL/min and aligned to one another with AIR (Woods *et al.*, 1992). Each subject's MR image was transformed into the stereotactic space of the human brain atlas (HBA) (Roland *et al.*, 1994) using linear and non-linear transformations, and the parameters were then used to transform the rCBF images into the same format. The normalized and aligned rCBF images were analysed using the general linear model (GLM), with condition, repetition and subject as factors (Fig. 4a). Three contrasts were tested: illusory versus fixation,

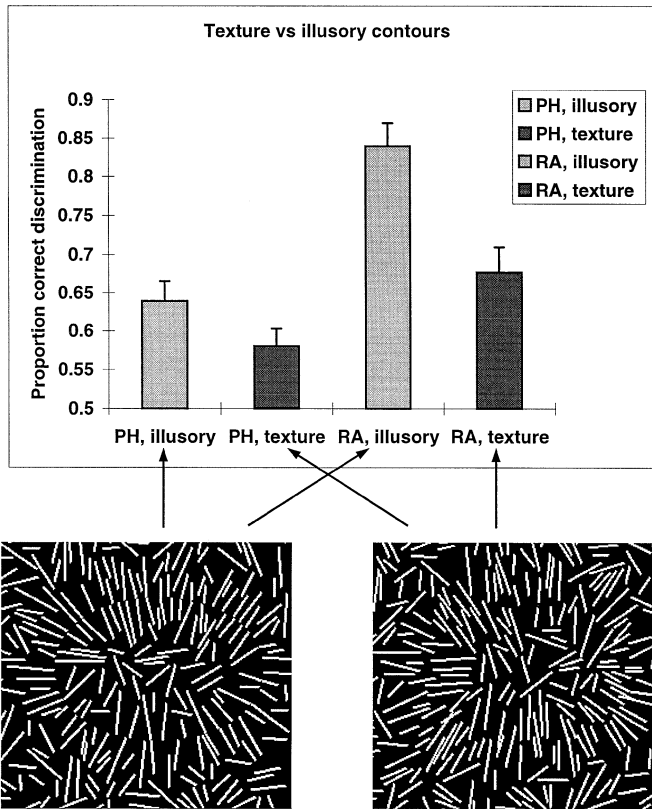


FIG. 3. Dependence on perception of illusory contours in the illusory condition for two subjects (PH and RA). Removal of illusory contours significantly ($P < 0.02$) reduces task performance in the illusory condition, demonstrating that the texture component of this stimulus is small.

real versus fixation, and illusory versus real. For each contrast, a t -image was calculated which was subsequently transformed into a Z -score image. Regions of significant clusters of activation in the Z -score images were determined using the CS method (Ledberg *et al.*, 1998). Five thousand simulations were made, based on the autocorrelation in 'signal-free' images (obtained by modelling the data so as to cancel out condition effects in the illusory–real contrast) (Fig. 4b). The Z -score images were thresholded at a Z -value of 3.9 and a minimum cluster size of $21 \times 2 \times 2$ mm voxels, corresponding to an estimated omnibus significance threshold $P < 0.05$.

To investigate condition-related changes in functional connectivity we also performed a principal component analysis (PCA) using the mean rCBF in selected regions of interest (ROIs). We selected these ROIs based on the following criteria: the ROI or its contralateral homologue should be activated by the illusory condition; and it should be definable anatomically or functionally. Two ROIs were defined functionally based on the comparison of the illusory condition with the real and fixation conditions (see Results): one in the right fusiform gyrus and one in the left pulvinar region. To account for possible subthreshold activations in the presumed contralateral homologues of these regions, we defined two additional ROIs by reflecting the functional regions across the midsagittal plane. Two more ROIs, V1 and V2, were defined anatomically as described below. Because there is little evidence of laterality (as opposed to retinotopy) in V1 and V2 we did not divide these ROIs into their left and right hemisphere components. Variance due to subject and repetition effects was removed by using the GLM to model the rCBF in all ROIs with

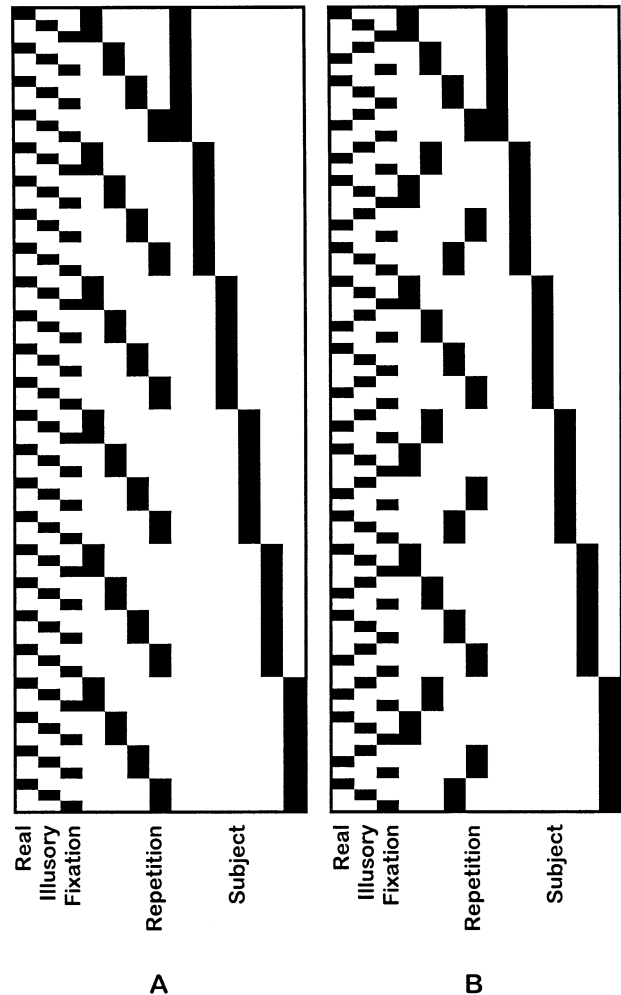


FIG. 4. Design matrices used for the generation of (a) statistical images and (b) signal-free images for measurement of the autocorrelation function (Ledberg *et al.*, 1998).

subject and repetition as factors. The residuals were then used as input for the PCA.

Anatomical delineation of V1 and V2

Cytoarchitectonic areas V1 and V2 were delineated in cell body-stained coronal sections of post-mortem brains. We examined histological serial sections of 10 human adult brains. The brains were fixed in 4% formalin or a Bodian's solution, embedded in paraffin, serially cut into coronal sections (20 μ m thick), and silver stained for cell bodies (Merker, 1983). High-resolution, three-dimensional FLASH scan MR images were obtained from all brains prior to the histological procedure, three-dimensionally reconstructed, and matched with the histological sections of the same brains (Schormann *et al.*, 1993, 1995; Geyer *et al.*, 1996; Schormann & Zilles 1997). This procedure compensates for shrinkage and distortion artefacts inevitably introduced by the histological procedure.

The borders of V1 and V2 were determined on each 60th section by a quantitative, observer-independent method (Schleicher *et al.*, 1999). This approach is based on the automated analysis of the grey level index (GLI) as a measure of the volume density of cell bodies (Schleicher *et al.*, 1995, 1999) (for applications see Geyer *et al.*, 1996; Amunts *et al.*, 1997) with a computer-controlled image analyser.

Profiles representing the laminar distribution of the GLI were determined from the border between layers I and II to the cortex/white matter boundary. These profiles covered the whole cortical region of interest tightly spaced and define the cytoarchitecture in quantitative terms. The observer-independent delineation is based on the comparison of neighbouring profiles in order to detect significant differences of their laminar pattern. Differences in the shape of the profiles were analysed by multivariate statistics (Mahalanobis distance and subsequent Hotelling's T2 test). Profiles sampled within a homogeneous cytoarchitectural area are similar and hence show low Mahalanobis distances between each other. Maximal distances occur between profiles which lie on opposite sides of an areal border. Borders were defined at those positions at which the distance measure was significant (Hotelling's T2 test, $P < 0.05$) (Amunts *et al.*, 1996; Schleicher *et al.*, 1999).

The cortical parcellations resulting from this procedure were then compared with classical cytoarchitectural criteria, especially with those described by von Economo & Koskinas (1925). Their area OC corresponds to V1, OB corresponds to V2 (Clarke & Miklossy, 1990; Zilles, 1990; Zilles & Clarke, 1997). Area V1 is characterized by a small cortical width, a generally high packing density of neurons, a clearly visible horizontal layering and the presence of a prominent layer IV, which can be further subdivided into layers IVA, IVB and IVC. The border between V1 and V2 is sharp and indicated by the abrupt disappearance of layer IVB (Gennari's stripe) and IVC of V1. Area V2 also shows a well-developed layering, but with a thin and not further subdivided layer IV, large pyramidal cells in layer III which decrease in size at the rostral boundary of V2, and a cell sparse layer (von Economo & Koskinas, 1925). The latter two features allowed differentiating between V2 and the rostrally adjoining area VP (ventral V3) and dorsal V3 (Clarke & Miklossy, 1990; von Economo & Koskinas, 1925). We found that the borders detected by the automated observer-independent approach were in precise correspondence with the borders defined by visual inspection on the basis of the classical, above-mentioned criteria. The Mahalanobis distances between profiles from V1 and V2 and between those from V2 and the rostrally adjoining cortex were significant in all sections and brains analysed.

The delineated regions were transformed into HBA brain space (Roland *et al.*, 1994) by automatic alignment and scaling of the MR image of each post-mortem brain to the standard brain of the HBA. This alignment was further improved by manual adaptation using linear and non-linear (asymmetric scale, skew, bend and local compression/expansion) transformations. Overlap (mean) images of each delineated area having a resolution of 1 mm^3 were made and median filtered with a 3 mm window to remove isolated voxels and reduce noise with minimal smearing. To determine appropriate thresholds for correct classification of each area we created a composite image of V1 and V2 in the following fashion:

$$C_i = \begin{cases} V_{i,V1} & \text{if } V_{i,V2} > 0 \text{ and } V_{i,V1} > V_{i,V2} \\ V_{i,V2} & \text{if } V_{i,V2} > 0 \text{ and } V_{i,V2} > V_{i,V1} \\ 0 & \text{otherwise} \end{cases} \quad (1)$$

where C_i is the label assigned to voxel i , and $V_{i,V1}$ and $V_{i,V2}$ the fraction of brains in which voxel i belongs to area V1 or V2, respectively. Thus, each voxel in the resulting image was labelled with the degree of overlap of either area V1 or V2, depending on which area had the highest overlap at that location. If V1 and V2 overlapped to the same degree, the voxel was assigned the label of the nearest unambiguously classified voxel. Such voxels were nearly all located at the boundary between V1 and V2. The resulting

classification is shown in Fig. 5. Inspection of this image showed that the border between V1 and V2 in the central regions corresponded approximately to the extent of these regions thresholded at 60% overlap (i.e. voxels which were classified as being in V1 or V2, respectively, in at least six out of the 10 brains). On this basis we defined the following classification criteria for delineating V1 and V2 for defining ROIs. For each brain voxel i ,

$$C_i = \begin{cases} V1 & \text{if } V_{i,V1} \geq 0.6 \text{ and } V_{i,V1} > V_{i,V2} \\ V2 & \text{if } V_{i,V2} \geq 0.6 \text{ and } V_{i,V2} > V_{i,V1} \\ \text{elsewhere} & \text{otherwise} \end{cases} \quad (2)$$

Voxels with equal overlap between V1 and V2 were classified as above. Assuming that anatomical variability is of similar magnitude across the width of V2 these criteria should provide a good estimate of the extent of V2 both caudally (along V1) and rostrally (along V3/VP).

According to previous anatomical (Clarke & Miklossy, 1990; Clarke, 1994a,b) and functional mappings (Sereno *et al.*, 1995; DeYoe *et al.*, 1996; Tootell *et al.*, 1996) of human extrastriate visual cortices, the upper and lower hemifield representations of human V2 are of equal width. In addition, both dorsal V3 and VP are well defined and relatively wider than they are in other primates (Sereno *et al.*, 1995). Thus, one would expect that if the cytoarchitectonic delineation of V2 also included dorsal V3 the volume of the dorsal part of this delineation would be substantially greater than the ventral part. As can be seen in Fig. 5, this is not the case. In a separate study (Larsson *et al.*, 1998) we have shown that this classification of V1 and V2 applied to individual inflated cortical surfaces (Dale & Sereno, 1993; Sereno *et al.*, 1995) consistently labels V1 along the calcarine sulcus and V2 as two stripes surrounding V1, each approximately half the width of V1. The anatomical delineations therefore provide reliable estimates of the location of V1 and V2 in HBA or Talairach space (Roland *et al.*, 1994; Talairach & Tournoux, 1988).

Results

Psychophysics

An ANOVA of subjects' responses during the real and illusory conditions showed a highly significant subject effect on both error rate (expressed as the proportion of incorrect responses, F ratio = 17.1; $P < 0.0001$) and reaction time (F ratio = 32.3; $P < 0.0001$). There was a weakly significant effect of condition on response times (F ratio = 5.66, $P < 0.05$; mean RTs: illusory 1220 ms; real 1180 ms), but error rates did not differ significantly. No other main effects or interactions were significant.

PET activations

Compared with the fixation condition, both the real and illusory conditions gave rise to highly significant and widespread activations in striate and extrastriate visual regions (Table 1, Fig. 6). The extrastriate activations extended ventrally along the fusiform and lingual gyri and dorsally within the cuneus with a smaller portion extending into the superior and inferior parietal lobules. The extent and size of these activations were very similar for both discrimination conditions. Comparison with the anatomical delineations of V1 and V2 showed that these activations included both V1 and V2 as well as more anterior extrastriate visual regions. The volume of the V1 and V2 ROIs constituted ~10 and 3% of the volume of these activations. The volume of the overlap between the activations and the maximum estimated extent of V1 [see Equation (1)] was 34%; the corresponding overlap with V2 was 26%. The visual activations extended much

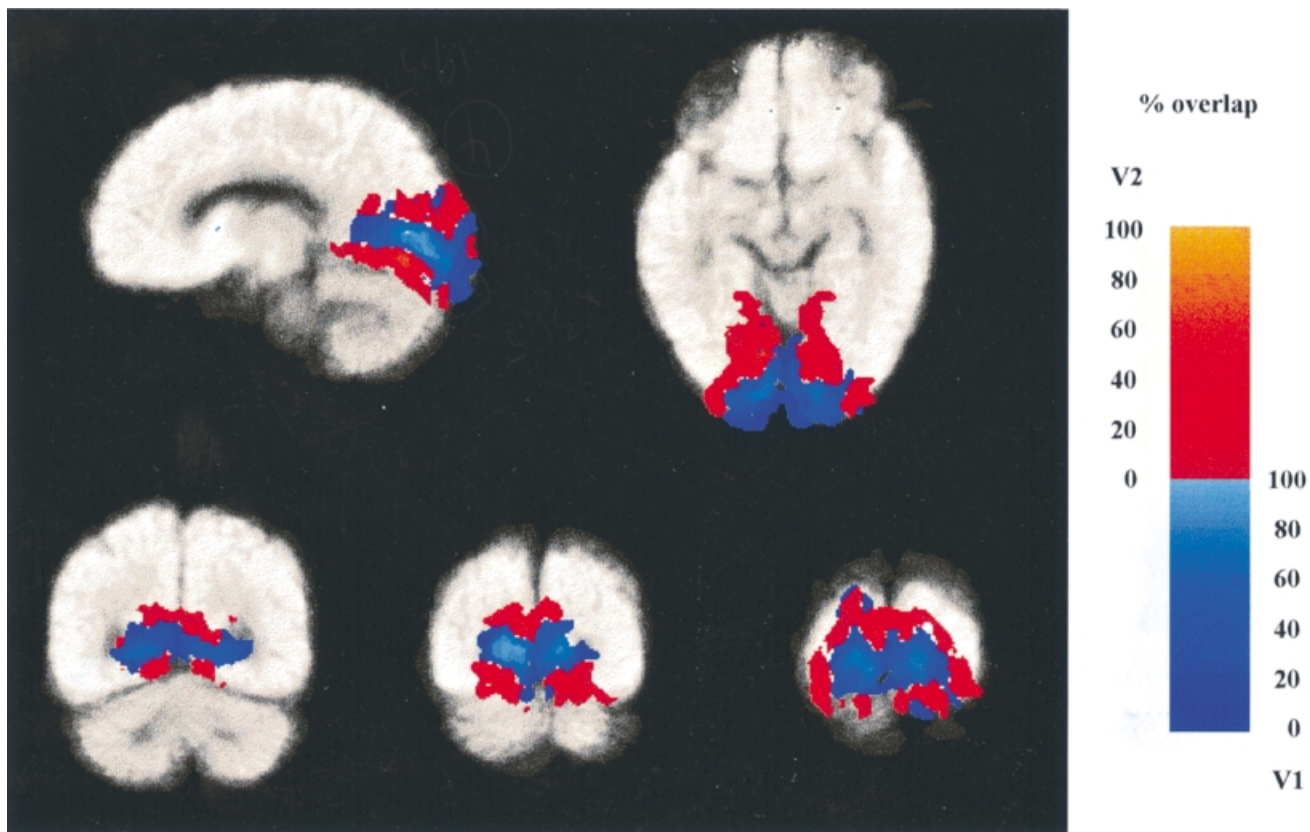


FIG. 5. Probability maps of V1 and V2. Average extent of V1 (blue) and V2 (red) determined by cytoarchitectural delineation in 10 post-mortem brains overlaid on the anatomically standardized average MR image of the individual brains. Sections shown are at $x = 10$, $z = -10$ (top), $y = -60$, -80 and -90 (bottom), respectively.

TABLE 1. Regions of significant rCBF increase during the illusory and real form discrimination conditions

Contrast	Location	Volume (mm ³)	Centre of gravity*		Mean z	Z-score	Significance†
			x	y			
Illusory–fixation	Striate and extrastriate posterior visual cortex	109 300	0	–80	–4	6.24	$P < 0.001$
	Left pulvinar complex	110	–22	–26	1	4.16	$P < 0.2$ (NS)
Real–fixation	Striate and extrastriate posterior visual cortex	103 600	0	–80	–3	6.15	$P < 0.001$
Illusory–real	Right fusiform gyrus	190	34	–70	–11	4.20	$P < 0.05$

*HBA coordinates (Roland *et al.*, 1994). Negative x coordinates denote locations left of the midline. †Omnibus significance of obtaining one or more false positive clusters of this size or larger as determined by CS analysis (Ledberg *et al.*, 1998).

further anterior, dorsal and lateral than the volume covered by the cytoarchitectonic areas. The activated regions therefore included extrastriate regions outside area V2. In addition to the activation of extrastriate visual cortex, there was a non-significant increase in the posterior part of the left thalamus, corresponding to the pulvinar complex (Talairach & Tournoux, 1988) in the illusory–fixation contrast. Because of the postulated role of the pulvinar in stimulus selection and visual attention (Robinson & Petersen, 1992), and the concern that the observed results may in part be due to attentional factors, we chose to include this region in the principal component analysis (see below), together with the corresponding region in the right hemisphere.

Only one region of activation, located in the right fusiform gyrus, was significant when contrasting the illusory and real conditions (Table 1, Fig. 6). This region was located well lateral to V1 and V2

and was part of the large volume activated in the illusory–fixation and real–fixation contrasts. No regions were significantly more activated by the opposite contrast (real–illusory). Neither V1 nor V2 showed any significant differences in rCBF between the real and illusory conditions, nor were there any significant changes in prefrontal cortical regions. The region in the fusiform gyrus showing a significant rCBF increase in the illusory condition together with its presumed contralateral homologue (obtained by reflection of the cluster across the midline) were used as ROIs in the principal component analysis.

Principal component analysis

The correlations between the different ROIs were generally weak and not significant (Table 2). Only V1 and V2 were significantly correlated both in the fixation ($r = 0.72$, $P < 0.0001$) and real

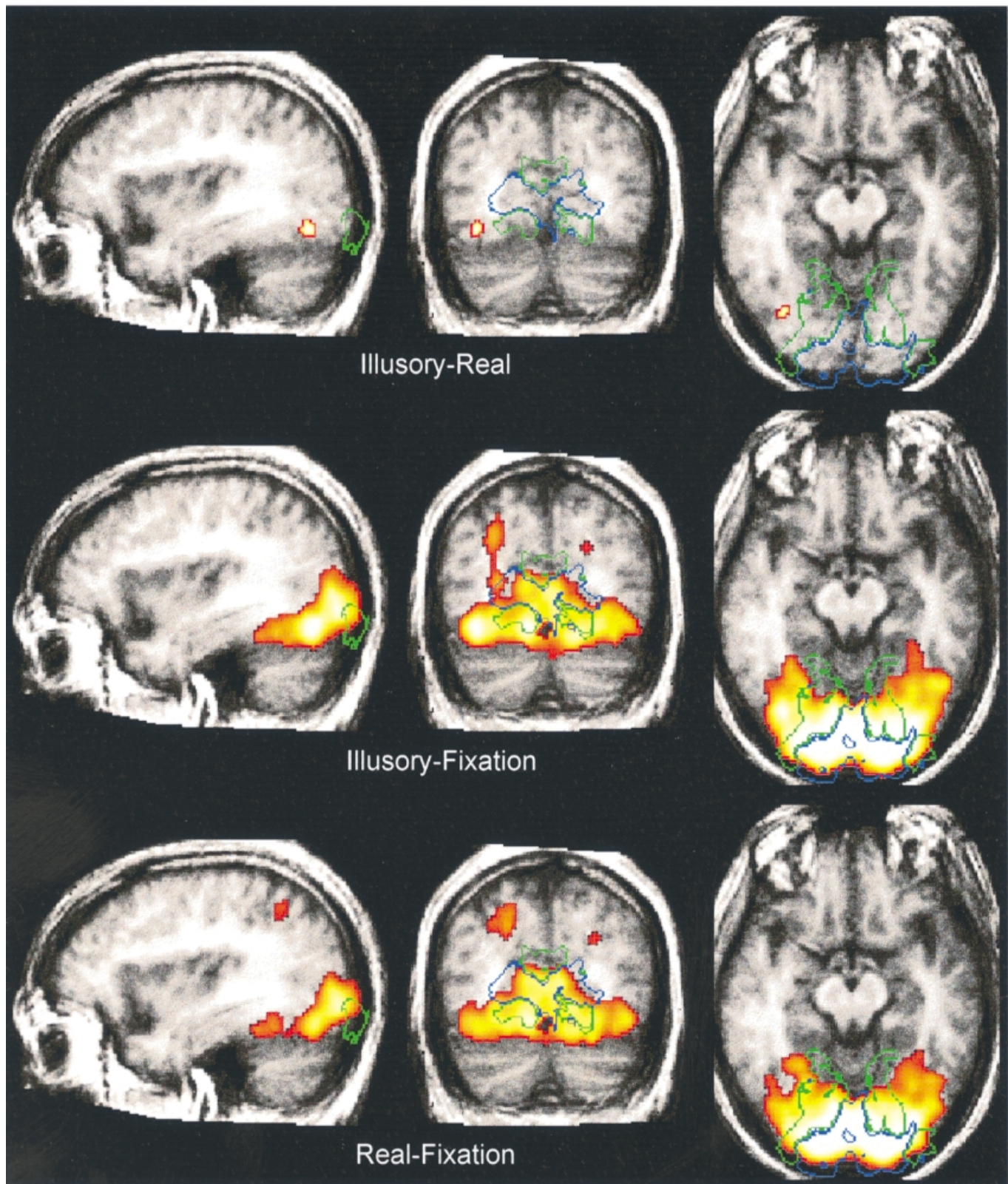


FIG. 6. Regions of significant rCBF increase during the illusory and real conditions. Significant activations (yellow-red) have been superimposed on the anatomically standardized average MR image of individual subjects' brains together with the boundaries of the maximum estimated extent of V1 (blue) and V2 (green) as defined in the text. The sections shown are located at $x=34$, $y=-71$, $z=-10$. Top, illusory-real; middle, illusory-fixation; bottom, real-fixation.

($r=0.57$, $P<0.005$) conditions, but this correlation was not significant in the illusory ($r=0.25$, $P>0.05$) condition. V2 was also

significantly negatively correlated ($r=-0.49$, $P<0.05$) with the left pulvinar ROI in the real condition only.

TABLE 2. Correlations of ROI rCBF residuals

ROI	Right fusiform	Left fusiform	Right pulvinar	Left pulvinar	V1	V2
Fixation condition						
Right fusiform	–	0.053	–0.19	–0.12	0.31	0.12
Left fusiform	0.053	–	–0.21	–0.18	–0.15	–0.069
Right pulvinar	–0.19	–0.21	–	–0.069	0.11	0.14
Left pulvinar	–0.12	–0.18	–0.069	–	–0.10	–0.28
V1	0.31	–0.15	0.11	–0.10	–	0.72***
V2	0.12	–0.069	0.14	–0.28	0.72***	–
Real condition						
Right fusiform	–	–0.37	–0.071	–0.19	–0.33	–0.13
Left fusiform	–0.37	–	–0.24	0.18	0.33	–0.16
Right pulvinar	–0.071	–0.24	–	0.19	–0.005	–0.042
Left pulvinar	–0.19	0.18	0.19	–	–0.31	–0.49*
V1	–0.33	0.33	–0.005	–0.31	–	0.57**
V2	–0.13	–0.16	–0.042	–0.49*	0.57**	–
Illusory condition						
Right fusiform	–	–0.34	–0.26	0.081	–0.35	–0.19
Left fusiform	–0.34	–	–0.12	0.36	0.35	–0.25
Right pulvinar	–0.26	–0.12	–	0.022	–0.25	–0.21
Left pulvinar	0.081	0.36	0.022	–	–0.14	–0.37
V1	–0.35	0.35	–0.25	–0.14	–	0.25
V2	–0.19	–0.25	–0.21	–0.37	0.25	–

Significance levels: * $P < 0.05$; ** $P < 0.005$; *** $P < 0.0001$ (uncorrected for multiple comparisons).

TABLE 3. Principal component analysis of ROI rCBF residuals

	PC1	PC2	PC3	PC4	PC5	PC6
Fixation condition						
Principal components						
Eigenvalue	1.95	1.35	1.09	0.75	0.64	0.22
Per cent	32.52	22.48	18.13	12.42	10.69	3.75
Cumulative per cent	32.52	55.01	73.13	85.56	96.25	100.00
Component loadings (ROI)						
Right fusiform	0.40	0.53	0.45	–0.53	0.26	0.10
Left fusiform	–0.15	0.70	–0.42	0.34	0.45	–0.02
Right pulvinar	0.21	–0.68	–0.43	–0.29	0.47	0.01
Left pulvinar	–0.39	–0.35	0.67	0.36	0.37	0.08
V1	0.89	–0.05	0.22	0.20	0.09	–0.33
V2	0.88	–0.06	–0.10	0.32	–0.08	0.32
Real condition						
Principal components						
Eigenvalue	1.98	1.62	1.15	0.58	0.43	0.23
Per cent	33.08	27.05	19.18	9.66	7.12	3.91
Cumulative per cent	33.08	60.13	79.31	88.97	96.09	100.00
Component loadings (ROI)						
Right fusiform	–0.35	–0.70	–0.31	0.46	0.28	0.04
Left fusiform	0.22	0.80	–0.35	0.35	–0.05	0.24
Right pulvinar	–0.19	–0.03	0.91	0.32	–0.12	0.10
Left pulvinar	–0.61	0.58	0.22	–0.13	0.48	–0.02
V1	0.86	0.22	0.14	0.27	0.18	–0.30
V2	0.82	–0.32	0.19	–0.21	0.27	0.27
Illusory condition						
Principal components						
Eigenvalue	1.74	1.67	1.23	0.62	0.44	0.30
Per cent	29.01	27.87	20.56	10.28	7.28	5.01
Cumulative per cent	29.01	56.87	77.43	87.71	94.99	100.00
Component loadings (ROI)						
Right fusiform	–0.65	–0.26	0.59	–0.15	0.23	0.29
Left fusiform	0.40	0.81	0.14	–0.07	–0.23	0.33
Right pulvinar	–0.28	0.13	–0.89	–0.02	0.26	0.21
Left pulvinar	–0.31	0.73	0.21	0.52	0.23	–0.11
V1	0.83	0.13	0.17	–0.23	0.45	–0.05
V2	0.54	–0.62	0.02	0.52	0.02	0.22

Loadings of >0.5 are printed in bold face for clarity.

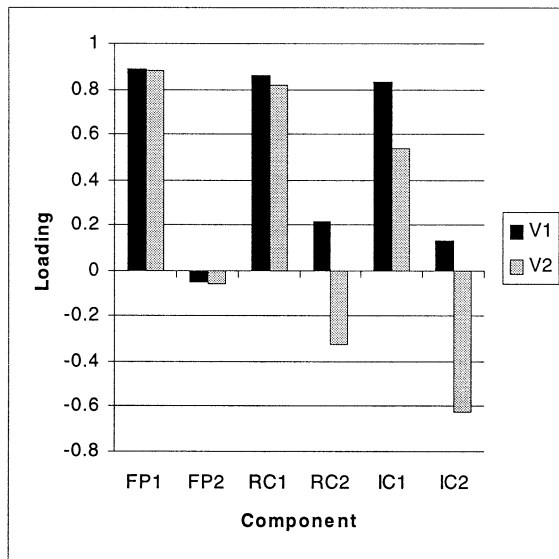


FIG. 7 Comparison of V1 and V2 loadings on the first and second principal components for each of the three experimental conditions (Fixation, Real and Illusory). F1 and F2, first and second principal components in the Fixation condition; R1 and R2, first and second principal components in the Real condition; I1 and I2, first and second principal components in the Illusory condition.

The principal component analysis identified three principal components (PCs) in each condition that had eigenvalues greater than one, which together accounted for nearly 80% of the variance in each condition. These components were quite distinct between conditions (Table 3, Fig. 7). In the fixation condition, the first PC could roughly be classified as early visual (V1 and V2). The second component loaded most strongly on the left and right fusiform regions and had a negative loading on the right pulvinar ROI. The third PC loaded mainly on the left pulvinar ROI.

In the real condition, the first PC also loaded primarily on V1 and V2, but in addition loaded negatively on the left pulvinar. The second PC loaded on the left and right fusiform regions and on the left pulvinar ROI. The loadings on the fusiform regions were of opposite sign.

The first two PCs in the illusory condition differed from those of the real and fixation conditions. Most notably, the loadings of V1 and V2 differed. V1 loaded strongly on the first PC, whereas the loading of V2 on this PC was markedly smaller than in the real or fixation conditions. Instead V2 loaded most strongly and negatively on the second PC, together with the left pulvinar and left fusiform regions (Fig. 7).

Discussion

Previous functional neuroimaging studies of illusory form perception have indicated that illusory and real contours are processed by similar regions in striate and extrastriate visual cortex, and that illusory form perception is not associated with activations of prefrontal cortex. The present study confirms and extends these findings for illusory contours defined by aligned line ends as opposed to the Kanizsa figures and abutting gratings used in earlier studies. The stimulus used in this study was designed to selectively activate the end-stopping cells believed to mediate illusory contour perception perpendicular to the inducer line orientation, while minimizing the textural and phase confounds present in illusory contours formed by phase-shifted gratings. In addition, by using closely matched stimuli

for real and illusory contours and a task which matched attention levels across these conditions, we were able to directly contrast real and illusory contour perception in the same subjects. Despite these differences in stimuli and analysis the main results of this study are in general agreement with previous studies. In particular, the results are consistent with the findings of Hirsch *et al.* (1995), who found that perception of illusory contours defined by Kanizsa figures activated regions of the cortex in the right fusiform gyrus. Because no stereotactic coordinates were published in that study it is, however, not possible to determine whether the illusory contour-specific activations reported by Hirsch *et al.* (1995) were located in the same region of the fusiform gyrus as the activation found in the present study. Collectively, the findings of these earlier studies and the present one suggest that although different types of illusory contours rely on different grouping mechanisms and may be modulated to different degrees by local and global features, the grouping processes take place in the same cortical regions, which overlap extensively with the cortical regions activated by perception of real contours.

We did not find any indication of illusory contour-specific activation of occipital visual cortex (anterior and lateral to V3A) as reported by Mendola *et al.* (1999). Negative findings in functional neuroimaging are inherently weak; yet, given the fact that attention was not controlled in the study of Mendola *et al.* (1999), and that the real and illusory stimuli used in that study differed strongly in salience, it cannot be excluded that those activations may have been due to attentional differences rather than reflecting a response specific to illusory contours. It is well known that attention can strongly modulate the activity of extrastriate visual cortex (Corbetta *et al.*, 1990; Corbetta *et al.*, 1991a,b; Wojciulik *et al.*, 1998). The difference in results may also reflect differences in stimuli, as Mendola *et al.* (1999) employed Kanizsa figures and phase-shifted gratings as opposed to the illusory contours induced by aligned line ends that were used in this study.

It has been postulated that because orientation-selective cells in V2 can respond to illusory contours (Peterhans & von der Heydt, 1989; von der Heydt & Peterhans, 1989), illusory contour perception should activate V2 more strongly than real contour perception, as suggested by the results of ffytche & Zeki (1996). However, these cells generally also respond to real contours which makes it unlikely that any differences should be observable at the population level. This is also what we found, i.e. that V2 is not specifically activated by illusory contours compared with real ones. Nonetheless, while both real and illusory stimuli activate early visual areas (V1 and V2) to the same degree, the principal component analysis indicates that the underlying mechanisms differ: illusory form perception is associated with a dissociation between the activity of V1 and V2 compared with perception of real contours or a visual control task. In the fixation and real conditions, V1 and V2 are significantly correlated with one another and load onto the same PCs. In contrast, in the illusory condition V1 and V2 are not significantly correlated and have their main loadings on different PCs. In other words, the illusory condition is associated with a partial decoupling of V1 and V2 activity compared with the real and fixation conditions. Bearing in mind that the small number of measurements limits the strength of the inferences that may be drawn from this observation, there are several possible explanations.

First, the effect may arise from differences in the local neuronal response properties in V1 and V2. It is known that neurons in macaque V2, but not in V1, respond to illusory contours (Peterhans & von der Heydt, 1989; von der Heydt & Peterhans, 1989). [One study (Grosf *et al.*, 1993) has reported cells that respond to illusory contours in V1, but the stimuli used in that study were not true

illusory contours, as they contained a luminance gradient along their entire length; illusory contours that do not contain such a continuous luminance gradient do not evoke responses in V1.] Luminance ('real') contours evoke orientation-selective responses both in V1 and V2. In the real and fixation conditions the visual percept corresponds directly to the luminance-defined contours which would be represented similarly by both V1 and V2 (assuming that human and macaque V1 and V2 have similar response properties). In contrast, the visual percept in the illusory condition is that of contours that have no physical counterpart; these contours would be represented in V2 but not in V1. Although the net effect of this difference may be too weak to be detected as a global change in activity, it is likely that the dissociation between stimulus and perception would be reflected in a change in the correlation of activity between V1 and V2. Second, using fMRI it has been shown that V2 can modulate V1 activity (Friston *et al.*, 1995). Changes in the strength of this modulation during illusory contour perception could in principle change the correlation of V1 and V2 in the manner observed. Third, V1 and V2 may be differentially modulated by feedback connections from higher level visual areas during perception of illusory contours. Modulation may be attentional in nature, serving to enhance the response to the perceived illusory figures rather than the inducer lines, or could be the result of a mechanism matching the visual input to a target template represented in higher visual regions (Ullman, 1995).

An obvious candidate for the origin of such top-down modulation is the region in the right fusiform gyrus which was more strongly activated by illusory than real contours. This region appears to correspond to the activated region described by Hirsch *et al.* (1995) who, using Kanizsa-type stimuli, found stronger activation of the right fusiform gyrus by illusory contours compared with real contours. The location of the activated region is lateral and anterior to V1 and V2. A comparison with a retinotopic mapping study of extrastriate visual areas (DeYoe *et al.*, 1996) suggests the region is located beyond retinotopic areas, lateral and anterior to human V4v. This region has been shown to be activated by a wide variety of complex visual stimuli, e.g. faces (Haxby *et al.*, 1994; Kanwisher *et al.*, 1997; Wojciulik *et al.*, 1998), animate and inanimate objects (Martin *et al.*, 1996), nonsense shapes (Schacter *et al.*, 1995) and even attention to relatively simple forms (Corbetta *et al.*, 1990), in addition to illusory contours (Hirsch *et al.*, 1995). Due to anatomical variability, even after anatomical standardization it is clearly possible that these strikingly different results arise from different loci and do not correspond to the same cortical region. Nevertheless, the great variety of stimuli that activate loci in this region argues against a simple interpretation of this activation as specifically subserving illusory contour perception or some related process, e.g. figure-ground segmentation. Instead it seems that this region is part of a larger area involved in general object recognition processing.

One reason for the stronger activation of this area during the illusory condition could be differences in attentional level between the real and illusory conditions. Attention has been shown to specifically modulate regions of extrastriate cortex in a stimulus-specific manner (Corbetta *et al.*, 1991a; Wojciulik *et al.*, 1998). Attentional differences might have been important if the shapes in the illusory condition were perceived to be less salient than the luminance-defined shapes in the real condition. The (non-significant) activation of the left pulvinar region in the illusory-fixation contrast might be taken as evidence of this, as the pulvinar has been shown to be important for attending to low salience stimuli (Robinson & Petersen, 1992) and has also been shown to be activated by tasks involving the perception of impossible (and therefore presumably attention-demanding) objects (Schacter *et al.*, 1995). However,

several facts argue against this interpretation. First, the conditions were closely matched for performance and salience as determined by prior measurement of detection times for illusory and real shapes. Second, there was no significant difference in the pulvinar region between the illusory and real conditions when directly contrasted. Third, the weak correlation between the left pulvinar region and the right fusiform region in the illusory condition suggests that the pulvinar and fusiform regions perform unrelated functions; thus, the fusiform activation cannot primarily be due to lower salience of the illusory shapes.

A possible explanation for the greater degree of activation during illusory form perception could be that perception of illusory contours requires top-down modulation of early visual areas by higher-order areas, e.g. the activated fusiform region. A change in the modulation of V1 and V2 during illusory contour perception need not be detectable in these areas as a global activity change, if they serve to re-route and fine-tune the activity of specific subpopulations of neurons without affecting the overall level of neuronal activity in these areas. Feedback from higher- to lower-order visual areas has been shown to be important for facilitation of responses to low salience features and suppression of responses to the surround (Lamme *et al.*, 1997; Hupé *et al.*, 1998); these processes might be particularly important for perception of illusory contours that would otherwise 'drown' in the background of real contours formed by the inducer lines. If illusory contours do indeed rely more strongly on top-down feedback mechanisms than do real contours, illusory contours should take longer to perceive than pure bottom-up, luminance-defined contours. This is consistent with the observed difference in response times between the real and illusory conditions, and could also account for the global activity change in the fusiform region. Longer processing times for illusory than real contours have also been demonstrated psychophysically for Kanizsa figures (Ringach & Shapley, 1996; Gegenfurtner *et al.*, 1997). Such data are suggestive, but given the lack of time resolution of the present PET data, any conclusions about the participation of the fusiform activation in feedback modulation of lower-order visual areas remain tentative. Further studies, using combined high-temporal and high-spatial resolution methods (e.g. combined EEG/fMRI), will be required to understand the temporal sequence of cortical activation during real and illusory form perception and the role of the fusiform region in these processes. The use of fMRI would also provide many more data points than PET, which would allow quantifying the nature of the coupling between V1 and V2 during real and illusory form perception.

Conclusion

We have shown that perception and discrimination of illusory forms formed by aligned line ends activate the same regions as those involved in perception of real forms. A subset of these regions, located in the right fusiform gyrus, is more strongly activated by illusory forms. The activation of a higher-order visual region suggests that illusory contour perception can involve both bottom-up feedforward and top-down modulatory mechanisms. These results extend and confirm previous neuroimaging studies of illusory contour perception using Kanizsa-type figures, and provide evidence that different kinds of illusory contours are processed by similar neuronal mechanisms. While the regions involved in real and illusory contour perception appear to overlap extensively, the patterns of correlations between V1 and V2 differ between the real and illusory contour conditions. This difference in functional connectivity probably reflects differences in the neuronal mechanisms underlying real and illusory contour perception.

Acknowledgements

This work was supported by grants from the Volvo Research Foundation, the Volvo Educational Foundation, and the Swedish Medical Research Council (MFR).

Abbreviations

FMRI, functional magnetic resonance imaging; HBA, human brain atlas; GLI, grey level index; GLM, general linear model; MR, magnetic resonance; PC, principal component; PET, positron emission tomography; rCBF, regional cerebral blood flow; ROI, region of interest.

References

- Amunts, K., Schlaug, G., Schleicher, A., Steinmetz, H., Dabringhaus, A., Roland, P.E. & Zilles, K. (1996) Asymmetry in the human motor cortex and handedness. *Neuroimage*, **4**, 216–222.
- Amunts, K., Schleicher, A., Schormann, T., Bürgel, U., Mohlberg, H., Uylings, H.B.M. & Zilles, K. (1997) The cytoarchitecture of Broca's region and its variability. *Neuroimage*, **5**, S353.
- Berkley, M.A., Debruyne, B. & Orban, G. (1994) Illusory, motion, and luminance-defined contours interact in the human visual system. *Vision Res.*, **34**, 209–216.
- Bravo, M., Blake, R. & Morrison, S. (1988) Cats see subjective contours. *Vision Res.*, **28**, 861–865.
- Clarke, S. (1994a) Association and intrinsic connections of human extrastriate visual cortex. *Proc. R. Soc. Lond. B: Biol. Sci.*, **257**, 87–92.
- Clarke, S. (1994b) Modular organization of human extrastriate visual cortex: evidence from cytochrome oxidase pattern in normal and macular degeneration cases. *Eur. J. Neurosci.*, **6**, 725–736.
- Clarke, S. & Miklossy, J. (1990) Occipital cortex in man: organization of callosal connections, related myelo- and cytoarchitecture, and putative boundaries of functional visual areas. *J. Comp. Neurol.*, **298**, 188–214.
- Corbetta, M., Miezin, F.M., Dobmeyer, S., Shulman, G.L. & Petersen, S.E. (1990) Attentional modulation of neural processing of shape, color, and velocity in humans. *Science*, **248**, 1556–1559.
- Corbetta, M., Miezin, F.M., Dobmeyer, S., Shulman, G.L. & Petersen, S.E. (1991a) Selective and divided attention during visual discriminations of shape, color, and speed: functional anatomy by positron emission tomography. *J. Neurosci.*, **11**, 2383–2402.
- Corbetta, M., Miezin, F.M., Shulman, G.L. & Petersen, S.E. (1991b) Selective attention modulates extrastriate visual regions in humans during visual feature discrimination and recognition. [Review]. *Ciba Foundation Symposium*, **163**, 165–175; discussion 175–180.
- Dale, A.M. & Sereno, M.I. (1993) Improved localization of cortical activity by combining EEG and MEG with MRI cortical surface reconstruction: a linear approach. *J. Cognit. Neurosci.*, **5**, 162–176.
- Davis, G. & Driver, J. (1994) Parallel detection of Kanizsa subjective figures in the human visual system [see comments]. *Nature*, **371**, 791–793.
- DeYoe, E.A., Carman, G.J., Bandettini, P., Glickman, S., Wieser, J., Cox, R., Miller, D. & Neitz, J. (1996) Mapping striate and extrastriate visual areas in human cerebral cortex. *Proc. Natl Acad. Sci. USA*, **93**, 2382–2386.
- Dresp, B. & Bonnet, C. (1995) Subthreshold summation with illusory contours. *Vision Res.*, **35**, 1071–1078.
- von Economo, C. & Koskinas, G. (1925) *Die Cytoarchitektur der Hirnrinde des erwachsenen Menschen*. Springer, Wien-Berlin.
- ffytche, D.H. & Zeki, S. (1996) Brain activity related to the perception of illusory contours. *Neuroimage*, **3**, 104–108.
- Friston, K.J., Ungerleider, L.G., Jezzard, P. & Turner, R. (1995) Characterizing modulatory interactions between areas V1 and V2 in human cortex: a new treatment of functional MRI data. *Hum. Brain Mapp.*, **2**, 211–224.
- Gegenfurtner, K.R., Brown, J.E. & Rieger, J. (1997) Interpolation processes in the perception of real and illusory contours. *Perception*, **26**, 1445–1458.
- Geyer, S., Ledberg, A., Schleicher, A., Kinomura, S., Schormann, T., Bürgel, U., Klingberg, T., Larsson, J., Zilles, K. & Roland, P.E. (1996) Two different areas within the primary motor cortex of man. *Nature*, **382**, 805–807.
- Grosz, D.H., Shapley, R.M. & Hawken, M.J. (1993) Macaque V1 neurons can signal 'illusory' contours. *Nature*, **365**, 550–552.
- Grossberg, S. (1994) 3-D vision and figure-ground separation by visual cortex. *Percept. Psychophys.*, **55**, 48–121.
- Gurnsey, R., Humphrey, G.K. & Kapitan, P. (1992) Parallel discrimination of subjective contours defined by offset gratings. *Percept. Psychophys.*, **52**, 263–276.
- Gurnsey, R., Poirier, F.J. & Gascon, E. (1996) There is no evidence that Kanizsa-type subjective contours can be detected in parallel. *Perception*, **25**, 861–874.
- Haxby, J.V., Horwitz, B., Ungerleider, L.G., Maisog, J.M., Pietrini, P. & Grady, C.L. (1994) The functional organization of human extrastriate cortex: a PET-rCBF study of selective attention to faces and locations. *J. Neurosci.*, **14**, 6336–6353.
- Heitger, F., Rosenthaler, L., von der Heydt, R., Peterhans, E. & Kubler, O. (1992) Simulation of neural contour mechanisms: from simple to end-stopped cells. *Vision Res.*, **32**, 963–981.
- von der Heydt, R. & Peterhans, E. (1989) Mechanisms of contour perception in monkey visual cortex. I. Lines of pattern discontinuity. *J. Neurosci.*, **9**, 1731–1748.
- von der Heydt, R., Peterhans, E. & Baumgartner, G. (1984) Illusory contours and cortical neuron responses. *Science*, **224**, 1260–1262.
- Hirsch, J., DeLaPaz, R.L., Relkin, N.R., Victor, J., Kim, K., Li, T., Borden, P., Rubin, N. & Shapley, R. (1995) Illusory contours activate specific regions in human visual cortex: evidence from functional magnetic resonance imaging. *Proc. Natl Acad. Sci. USA*, **92**, 6469–6473.
- Hupé, J.M., James, A.C., Payne, B.R., Lomber, S.G., Girard, P. & Bullier, J. (1998) Cortical feedback improves discrimination between figure and background by V1, V2 and V3 neurons. *Nature*, **394**, 784–787.
- Kanwisher, N., McDermott, J. & Chun, M.M. (1997) The fusiform face area: a module in human extrastriate cortex specialized for face perception. *J. Neurosci.*, **17**, 4302–4311.
- Lamme, V.A.F., Zipser, K. & Spekreijse, H. (1997) Figure-ground signals in V1 depend on consciousness and feedback from extra-striate areas. *Soc. Neurosci. Abstr.*, **23**, 1543.
- Larsson, J., Amunts, K., Gulyas, B., Malikovic, A., Zilles, K. & Roland, P.E. (1998) Functional and anatomical delineation of human visual areas: a multiple-criteria approach. *Neuroimage*, **7**, S305.
- Ledberg, A., Åkerman, S. & Roland, P.E. (1998) Estimation of the probabilities of 3D clusters in functional brain images. *Neuroimage*, **8**, 113–128.
- Martin, A., Wiggs, C.L., Ungerleider, L.G. & Haxby, J.V. (1996) Neural correlates of category-specific knowledge. *Nature*, **379**, 649–652.
- Mendola, J.D., Dale, A.M., Fischl, B., Liu, A.K. & Tootell, R.B.H. (1999) The representation of illusory and real contours in human cortical visual areas revealed by functional magnetic resonance imaging. *J. Neurosci.*, **19**, 8560–8572.
- Merker, B. (1983) Silver staining of cell bodies by means of physical development. *J. Neurosci. Meth.*, **9**, 235–241.
- Meyer, E. (1989) Simultaneous correction for tracer arrival delay and dispersion in CBF measurements by the H2150 autoradiographic method and dynamic PET. *J. Nucl. Med.*, **30**, 1069–1078.
- Paradiso, M.A., Shimojo, S. & Nakayama, K. (1989) Subjective contours, tilt aftereffects, and visual cortical organization. *Vision Res.*, **29**, 1205–1213.
- Peterhans, E. & von der Heydt, R. (1989) Mechanisms of contour perception in monkey visual cortex. II. Contours bridging gaps. *J. Neurosci.*, **9**, 1749–1763.
- Peterhans, E. & von der Heydt, R. (1991) Subjective contours – bridging the gap between psychophysics and physiology. *Trends Neurosci.*, **14**, 112–119.
- Ringach, D.L. & Shapley, R. (1996) Spatial and temporal properties of illusory contours and amodal boundary completion. *Vision Res.*, **36**, 3037–3050.
- Robinson, D.L. & Petersen, S.E. (1992) The pulvinar and visual salience. [Review] [47 refs]. *Trends Neurosci.*, **15**, 127–132.
- Roland, P.E., Graufelds, C.J., Wählin, J., Ingelman, L., Andersson, M., Ledberg, A., Pedersen, J., Åkerman, S., Dabringhaus, A. & Zilles, K. (1994) Human brain atlas: for high resolution functional and anatomical mapping. *Hum. Brain Mapp.*, **1**, 173–184.
- Schacter, D.L., Reiman, E., Uecker, A., Polster, M.R., Yun, L.S. & Cooper, L.A. (1995) Brain regions associated with retrieval of structurally coherent visual information. *Nature*, **376**, 587–590.
- Schleicher, A., Amunts, K., Geyer, S., Morosan, P. & Zilles, K. (1999) Observer-independent method for microstructural parcellation of cerebral cortex: a quantitative approach to cytoarchitectonics. *Neuroimage*, **9**, 165–177.
- Schleicher, A., Amunts, K., Geyer, S., Simon, U., Zilles, K. & Roland, P.E. (1995) A method of observer-independent cytoarchitectonic mapping of the human cortex. *Hum. Brain Mapp.*, **1** (Suppl.), 77.

- Schormann, T., Dabringhaus, A. & Zilles, K. (1995) Statistics of deformations in histology and application to improved alignment with MRI. *IEEE Trans. Med. Imaging*, **14**, 25–35.
- Schormann, T.V., Matthey, M., Dabringhaus, A. & Zilles, K. (1993) Alignment of 3-D brain data sets originating from MR and histology. *Bioimaging*, **1**, 119–128.
- Schormann, T. & Zilles, K. (1997) Limitations of the principal-axes theory [letter]. *IEEE Trans. Med. Imaging*, **16**, 942–947.
- Sereno, M.I., Dale, A.M., Reppas, J.B., Kwong, K.K., Belliveau, J.W., Brady, T.J., Rosen, B.R. & Tootell, R.B. (1995) Borders of multiple visual areas in humans revealed by functional magnetic resonance imaging. *Science*, **268**, 889–893.
- Shipley, T.F. & Kellman, P.J. (1992) Strength of visual interpolation depends on the ratio of physically specified to total edge length. *Percept. Psychophys.*, **52**, 97–106.
- Smith, A.T. & Over, R. (1979) Motion aftereffect with subjective contours. *Percept. Psychophys.*, **25**, 95–98.
- Soriano, M., Spillmann, L. & Bach, M. (1996) The abutting grating illusion. *Vision Res.*, **36**, 109–116.
- Talairach, J. & Tournoux, P. (1988) *Co-planar Stereotaxic Atlas of the Human Brain*. Thieme, Stuttgart.
- Tootell, R.B., Dale, A.M., Sereno, M.I. & Malach, R. (1996) New images from human visual cortex. *Trends Neurosci.*, **19**, 481–489.
- Ullman, S. (1995) Sequence seeking and counter streams: a computational model for bidirectional information flow in the visual cortex. *Cerebr. Cortex*, **5**, 1–11.
- Vogels, R. & Orban, G.A. (1987) Illusory contour orientation discrimination. *Vision Res.*, **27**, 453–467.
- Wojciulik, E., Kanwisher, N. & Driver, J. (1998) Covert visual attention modulates face-specific activity in the human fusiform gyrus: fMRI study. *J. Neurophysiol.*, **79**, 1574–1578.
- Woods, R.P., Cherry, S.R. & Mazziotta, J.C. (1992) Rapid automated algorithm for aligning and reslicing PET images. *J. Comput. Assist. Tomogr.*, **16**, 620–633.
- Zilles, K. (1990) Cortex. In Paxinos, G. (ed.), *The Human Nervous System*. Academic Press, San Diego, pp. 757–802.
- Zilles, K. & Clarke, S. (1997) Architecture, connectivity and transmitter receptors of human extrastriate cortex. Comparison with non-human primates. In Rockland, K. S., Kaas, J. H. & Peters, A. (eds), *Cerebral Cortex: Extrastriate Cortex in Primates*. Plenum Press, New York, pp. 673–742.